

Modeling the Offset Solid-Ink Printing Process

Trevor Snyder and Steve Korol
Tektronix Color Printing and Imaging Division
Wilsonville, OR 97070

Abstract

Over the last few years, solid ink technology has emerged as a key player in the office color, prepress proofing, and wide format color printing markets. The success of this technology stems largely from its combination of ink jet printing with inks relying on solidification rather than colorant vehicle evaporation to achieve image fixation. The following paper offers the reader a more detailed explanation of solid ink printing technology through the presentation of thermal and mechanical image formation models. The thermal model presented solves the transient temperature distribution for single hemispherical ink droplets including the droplets change of state from liquid to solid. The model is used to study the solidification time and transient temperature distribution of single pixel ink droplets, including the effects of remelting. The mechanical model presented solves for the stress, strain, and deflection distributions in the transfix nip. Both the macroscopic (nip sized) and microscopic (pixel sized) nip characteristic requirements are presented.

Introduction

The most prevalent ink jet printer architecture is the *direct* jetting type. In this architecture the printhead shuttles back and forth across the width of the page, progressively jetting an image down the length of the page as the media passes beneath the printhead. In this implementation, the ink is jetted directly onto the final receiver media. Many different types of solid and liquid inks have been used in this application. In a second ink jet printing architecture, known as the *transfer* or *offset* ink jet printing process, the printhead jets an image first onto an intermediate transfer drum. After the complete image has been deposited on the transfer drum, the media is brought into contact with the

drum through a high-pressure nip and the image is transferred onto the media. This process is not unlike a conventional *offset* printing press. This relatively new printing process is outlined in U.S. patents 5372852 and 5389958 and is the topic of this paper.

Figure 1 illustrates the Tektronix solid-ink offset printing process, as employed by the Tektronix Phaser® 350 color printer.

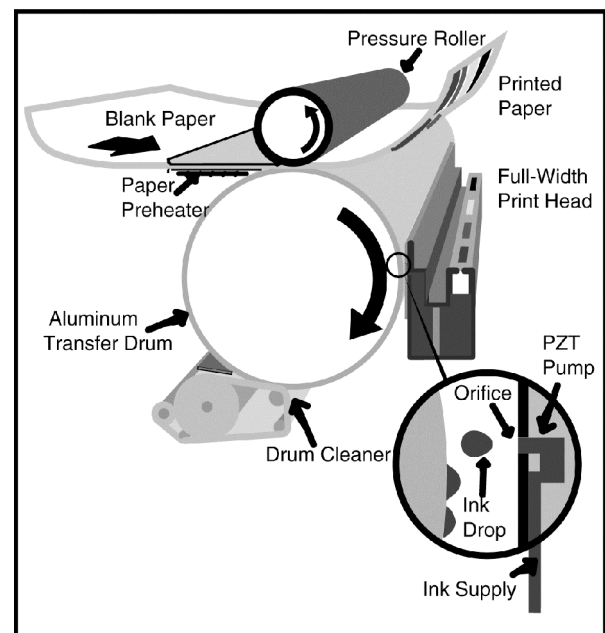


Figure 1: Tektronix Solid Ink offset printing process.

In this implementation of the technology, a proprietary *solid*, or *hot melt*, ink is placed into a heated reservoir where it is maintained in a liquid state. This highly engineered ink is formulated to meet a number of constraints, including low viscosity at jetting temperatures, specific viscoelastic

properties at drum-to-media transfer temperatures, and high durability at room temperatures. Once within the printhead, the liquid ink flows through manifolds to be ejected from microscopic orifices through use of proprietary piezoelectric transducer (PZT) printhead technology. The duration and amplitude of the electrical pulse applied to the PZT is very accurately controlled so that a repeatable and precise pressure pulse can be applied to the ink, resulting in the proper volume, velocity, and trajectory of the droplet. Four rows of jets are used in the current printhead, each row representing a unique color. The individual droplets of ink are jetted onto a liquid layer, which is supported by a rotating anodized aluminum drum. The drum and liquid layer are held at a specified temperature such that the ink hardens to a ductile viscoelastic state. After the entire image has been jetted onto the liquid layer on the drum, it is transferred and fixed, or *transfixed*, onto pre-heated receiver media. A high durometer synthetic pressure roller, when placed against the aluminum drum, develops a high-pressure nip which compresses the paper and ink together, spreads the ink droplets, and fuses the ink droplets into the media.

The system is a true plain-paper process, in that common office copier papers can be used to yield brilliant color prints; however, increased durability and image quality can be achieved when proprietary receiver media coatings are employed. These coatings promote physical and/or chemical interactions between the ink and the media surface. The key advantages of the offset solid-ink printing process in the office color market are ease of use, print quality, color consistency, media flexibility, low cost per copy, and excellent transparency quality. A medical diagnostic printer using this technology is presently under development having the additional benefits of a dry hard copy system, relatively low size and weight, high maximum optical density, multiple media size capability, and plain paper printing capability.

To achieve optimal image quality, several subsystems must work in conjunction. The goal of the current paper is to present a qualitative overview of the transient temperature distribution of the ink droplets during solidification, and to present an overview of the required transfixing in order to achieve optimal image quality.

Solid-Ink Drop Solidification Model

Description of Model

Deposition of a single, isolated ink droplet on the transfer drum surface can be broken down into five discrete steps. In the first step the droplet is ejected from the printhead. In the second step, the droplet, with proper mass, velocity, and trajectory, flies toward the transfer drum. During flight, the droplet remains nearly uniform temperature but changes shape significantly, as the forces of

surface tension work to pull the droplet into a spherical shape. The third step is dissipation of kinetic energy via impact of the droplet on the drum surface. The fourth step is physical droplet spread immediately following impact. For spreading to take place, the thermal energy from the droplet must heat the drum surface as the outer edge advances. The fifth and final step is droplet solidification, which occurs once enough of the droplet's thermal energy has dissipated in order to keep the temperature of the substrate above the solidification temperature at the advancing edge. The distortion of the droplet after impact has been calculated using the following approximate equation,

$$\frac{S}{D} = 1.26 * (1 + C_2 * \sqrt{Re})^{1/3}$$

where the S is the spot size (diameter), D is the equivalent drop diameter of the same volume, Re is the Reynolds number for the drop and C_2 is a constant of integration equal to approximately 0.5. This equation was given by Wright, 1992 and predicts a spot size about two times the diameter of the sphere of equivalent volume. The transfer drum's relative high thermal mass and low temperature relative to the droplet's solidification temperature reduce the amount of thermal spreading so that an appropriate spot size approximation can be made by computing the diameter of a hemisphere of volume equal to that of the droplet. The validity of this approximation was verified by analyzing digitally captured images of single droplets impacting the media surface. These images are presented in Figure 2. Note the substantially hemispherical shape of the drop following impact. It was observed that the droplet did not continue to spread significantly once this hemispherical shape was achieved.

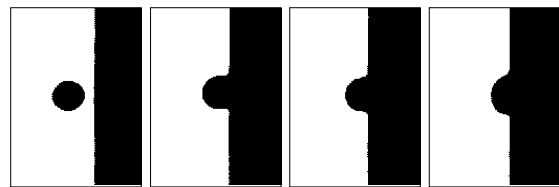


Figure 2: High-speed digital micrography of droplet impacting the media surface.

The solidification model consists of two parts. The first part solves the transient heat transfer problem involving the solidification of a liquid ink droplet. The droplet, initially at a uniform temperature above the ink's melting temperature, is jetted onto the liquid layer on the aluminum transfer drum that is also initially at uniform temperature. This portion of the model is designed to simulate the placement of individual droplets onto the drum. The second part of the model solves the same transient heat transfer problem for a single liquid ink droplet; however, the receiver media is ink

rather than aluminum. This is designed to simulate the placement of individual ink droplets onto ink previously deposited on the drum, as in the case of secondary colors produced by superimposing two primary colors (i.e. cyan on top of magenta to yield blue). For simplicity, the medium on which the droplet is placed will simply be referred to as the substrate material and will be either aluminum or ink. The solution of problems such as this are inherently difficult because the interface between the solid and liquid phases is moving as the latent heat is absorbed at the interface. The location of the solid-liquid interface is not known *a priori* and must follow as part of the solution. The solution used the fully implicit finite difference method, which was formulated using the energy balance approach. While the model was formulated for any number of nodes, the results presented in this report are for 200 nodes in the droplet and 200 nodes in the receiver material.

Validity of Model

As mentioned earlier, the high thermal mass and relatively low temperature of the transfer drums result in very little thermal spreading of the droplet following impact. The value of the Bond number for an individual ink droplet, given its surface tension and size, also dictates that the pixel shape is gravity independent. The assumed hemispherical geometry has the minimum surface area for a given periphery and volume. However, this single pixel approach is not valid for many of the pixels in the actual offset phase-change printing process. The Tektronix Phaser® 350 printer provides dot size modulation to switch between a 300-dip pixel and a 600-dpi pixel at jetting frequencies of 11 and 8 kHz, respectively. Therefore, the time scale between neighboring drops is much smaller than the solidification time. The extremely small time between the placement of neighboring droplets results in their complete coalescence. In many cases, this results in the formation of lines of ink instead of individual droplets of ink. Figure 3 shows a single solidified droplet and a solidified and coalesced line of pixels as they appear on the transfer drum prior to transfix.

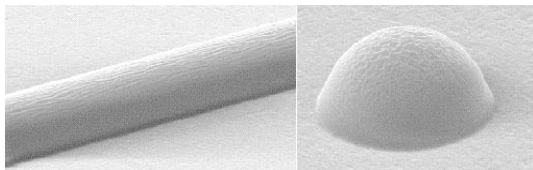


Figure 3: SEM images of single droplet and line of droplets after solidification, prior to transfixing.

To verify the capability of the model to predict single droplet solidification, a series of single droplet width lines were printed at various jetting frequencies. Controlling the jetting frequency controlled the placement time between neighboring droplets. At very fast jetting frequencies, the

placement time between neighboring droplets was much smaller than the solidification time of the droplets, allowing complete coalescence of adjacent droplets on the drum. In contrast, at very slow jetting frequencies, the placement time between neighboring droplets was much larger than the solidification time of the droplets, resulting in a complete lack of coalescence between adjacent droplets. Assuming that coalescence of adjacent droplets will occur only when the outer droplet shell is substantially fluid, varying the droplet deposition rate in this way allowed a bound to be drawn on the solidification time for single droplets. It was determined that the difference between the observed and predicted solidification times were within about 5%. Figure 4 presents SEM images of a single droplet width non-coalesced line, a partially coalesced line, and a completely coalesced line from the testing.

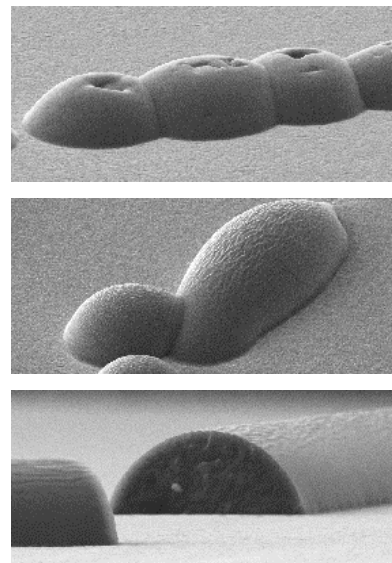


Figure 4: Non-coalesced, partially coalesced, and completely coalesced single droplet width lines.

Single Droplet Solidification

Figure 5 shows three temperature distribution maps of a single ink droplet on an aluminum substrate as calculated by the model. The receiver (transfer drum) and ink height is shown on one axis with the width on the other axis. Three time steps are shown: an initial time slice immediately following droplet impact showing some solidification, an intermediate time slice showing partial solidification, and a final time slice showing near complete solidification. The temperature scale is shown on the right side of each of the images.

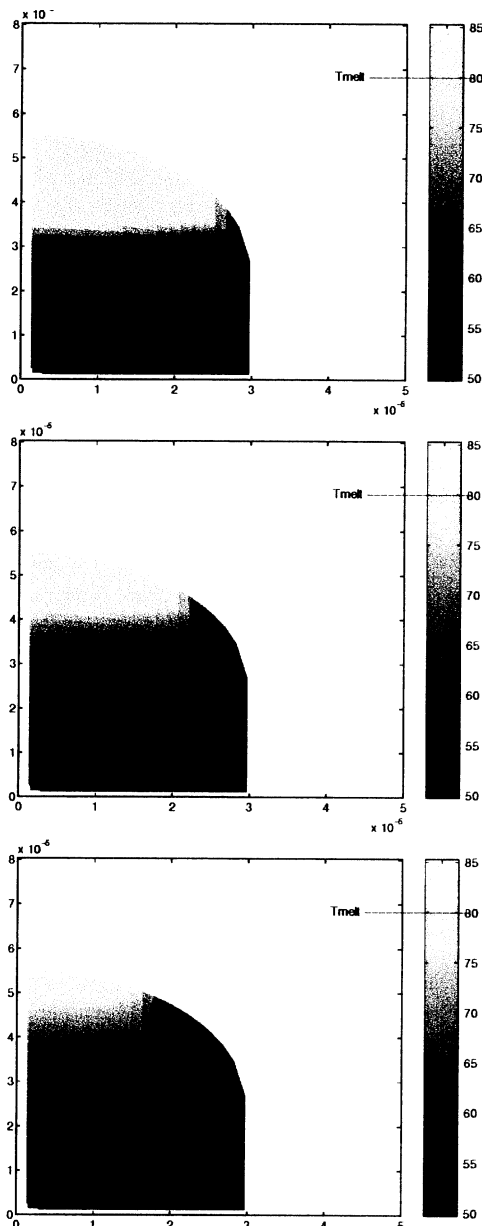


Figure 5: Temperature maps of single pixels during solidification on an aluminum receiver.

The relatively high thermal mass and conductivity of the aluminum drum (which supports the liquid layer on which the droplets are placed) compared to the ink droplets themselves, led to only a slight temperature drop at the drum surface. As might be expected, the base and edges of the of the ink droplet solidify before the center. Note that the solidification front moved from both the base and sides of the droplet. This resulted in solidification of the droplet edge in close proximity to the drum well before the edge at the top of the droplet. In general, the center and top of the droplet was the last to solidify for all the tests performed with droplet diameters on the order of 40 to 100 μm . However, droplets much larger than these were found to

solidify completely at the outer shell prior to the core of the droplet. Also, while not shown in this paper, the solidification time on non-metallic media such as a plastic film or paper (say, in a traditional direct-printing architecture) would be quite different. The relatively lower thermal mass of these receiver materials results in a significant temperature increase of the substrate and a corresponding increase in the solidification time.

The solidification program was run for a number of different drop masses and five substrate temperatures. Figure 6 plots the normalized solidification time as a function of the normalized drop mass and the actual substrate temperature. The solidification time is on the order of 10-100ms, however, for purposes of publication, we normalized the plot for both the time and drop mass. This was accomplished by simply dividing the drop mass by the maximum drop mass in the tests and the solidification time by the maximum solidification time calculated in the tests. Therefore, the plots range from zero to one. The plot was constructed based on complete solidification of the droplet, including its core. Note first and foremost the obvious trend toward increasing solidification time with substrate temperature and droplet size. Note further the strong non-linear dependence of the solidification time with substrate temperature. At medium to low substrate temperatures, the solidification time is not as strong a function of the temperature as at higher substrate temperatures.

The amount the drop can spread is a function of the ability of the drop to heat the substrate at its leading edge. At higher drum temperatures this heating takes less energy and the droplets will spread much more. As the droplet spreads, the maximum thickness of the droplet decreases. This provides a smaller thermal resistance for heat transfer. Therefore, the results shown in Figure 6 at the higher drum temperatures are probably slightly higher than actual

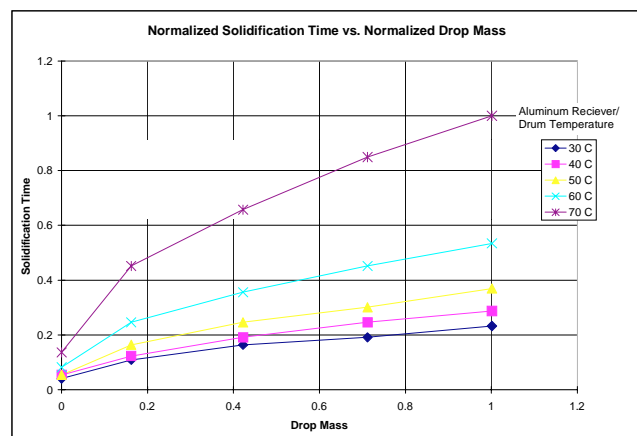


Figure 6: Trend of solidification time as a function of the drop mass and the substrate temperature.

Single Droplet Solidification with Remelting

Another interesting case predicted by the model occurs when a droplet is jetted onto an ink surface pre-existing on the drum. This situation is common in a subtractive color printer where secondary colors are produced by overlaying droplets of various translucent colors. In this case, we define the *remelt zone* as that region of the pre-deposited droplet that has remelted due to the influence of an ink droplet jetted onto its surface. Figure 7 presents a map of the temperature distribution of a single ink droplet on an ink receiver surface as calculated by the model. The time slice shown is just after the droplet has impacted the pre-deposited ink layer and the remelt zone has reached its maximum growth. It was assumed that the pre-deposited ink is at the drum temperature. The depth of the remelt zone was calculated to be about 10% of the pixel height. Due to the large latent heat involved and the small thermal conductivity and capacity of the ink, the depth of the remelt zone was not a strong function of the initial temperature of the primary ink layer, i.e., the drum temperature. The solidification time in this case represented a large increase over that calculated with an aluminum substrate. This increase was due mainly to the insulating effects of the ink, with its much lower thermal conductivity and thermal mass compared to the aluminum transfer drum.

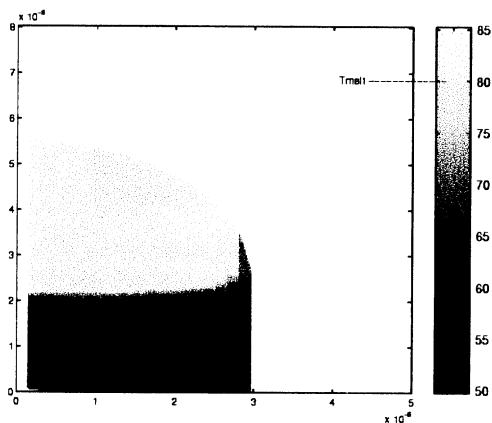


Figure 7: Temperature map of a single pixel during solidification with remelting on an ink substrate.

Solid-Ink Transfix Model

To this point, we have discussed only the solidification of ink droplets on the intermediate transfer drum. In order to gain an understanding of the complete offset solid-ink imaging process, we must consider transfer and fusing, or *transfixing*, of the ink on the drum to the final receiver media. During transfix, the ink and media are compressed between the transfer drum and a high durometer synthetic pressure roller, referred to as the *transfix roller*. Transfixing spreads the ink droplets and fuses them into the media.

Two important aspects of the transfix process are the micro-scale and macro-scale pressure distributions and conformances. The macro-scale conformance is measured by the width of the nip formed between the transfer drum and the transfix roller. The conformance is controlled by

the transfix roller geometry and material properties. The pressure distribution is controlled by both the transfix roller geometry and material properties as well as the load used during the transfix. The micro-scale conformance is controlled by a combination of the transfix roller geometry and material properties, and the media thickness, material properties and surface characteristics. The dependence of the media on the small-scale conformance results from the fact that the ink pixels are on the drum side of the media and not on the roller side. Therefore the media itself forms a barrier between the roller and the pixels.

To study transfix process requirements, a nip model was developed. A two-dimensional analysis of a radial slice across two parallel cylindrical rolls allowed the study of macro-scale aspects of the transfix nip. Analysis included prediction of the pressure profile across the nip, the width of the nip, the average stress across the nip, and stress and strain plots for the nip region. Figure 8 shows the pressure distribution calculated from the numerical model for a transfix roller against an aluminum transfer drum.

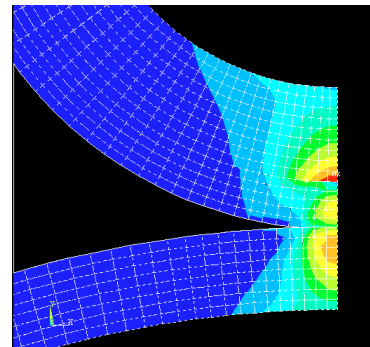


Figure 8: Deflection and stress distribution of a transfix roller and transfer drum nip.

A two-dimensional analysis of an axial slice through the centerlines of two cylindrical rolls allowed the study of micro-scale aspects of the transfix process. In this case, an ink droplet is placed between the two rolls along with a separate layer to account for the media. The model predicts the gap between the outside surfaces of the rolls in the region not covered by the ink droplet. The average pressure from the macro-scale model was used as an input to the micro-scale model. An example of this analysis is given in Figure 9, where material deflection and pressure distribution are plotted for the region immediately surrounding a single ink droplet during transfix. Note that the high-pressure nip has substantially flattened the droplet from its hemispherical initial condition. Note further the partial conformance of the receiver media (the upper surface) to the droplet.

The macro-scale and micro-scale nip characteristics have a significant impact on the amount of pixel spreading (dot gain) during transfix. Pressure control across the length of the nip is also critical to insure a uniform dot gain is achieved. Also, to a large extent, the nip characteristics control the dot loss (the number of ink droplets left on the drum after transfix). However, the influenced of the surface topography of the media also plays a role. Additionally, the case of two overlaid droplets results in about twice the ink

layer thickness with a corresponding disparity in conformance between the area immediately adjacent to the thick ink layer and the receiver media. Therefore, the most difficult case for the transfix process is that in which single layer droplets are placed next to, but not contacting, double layer droplets, with the intent to transfix the droplets onto a rough, non-conforming receiver media.

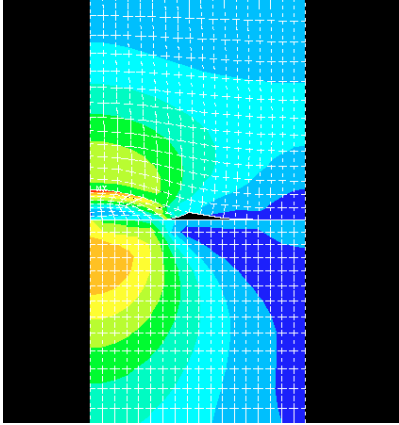


Figure 9: Deflection and stress distribution of a single pixel within the transfix nip.

Design of the nip as described here, along with the optimization of many other process variables allows the offset solid-ink process of the Phaser® 350 printer to produce continuous solid-fill densities across the entire printed page. Also, the transfix efficiency of the Phaser® 350 printer approaches 100% for most practical images. For the medical diagnostic market a proprietary digital halftoning algorithm will be used which maintains at least one drop in the printed resolution matrix which allows 100% image transfer in every image.

Summary and Conclusion

The models presented predicts droplet solidification time and transfix characteristics given a number of input parameters. These variables were chosen as key response variables through analysis of the entire printing system. This is not to say that if we were to optimize these two responses, excellent images would result, but rather that they play a key role in the formation of high quality images. Several other variables, the details of which are well beyond the scope of this paper, must be considered in order to produce a truly complete model of the offset solid ink printing process. Examples of some of the variables contributing to image quality include printhead ink droplet jetting (the pixel size and shape), thermal spreading, drum temperature, media preheat temperature, dwell time in the nip (the transfix velocity and nip width), digital halftoning, and the mechanical motion control systems. Interestingly, many of these variables effect droplet solidification time and transfix efficiency. In order to illustrate the effects of a couple of these variables on image noise, Figure 10 presents SEM images of solidified ink droplet lines on the transfer drum, prior to transfix.

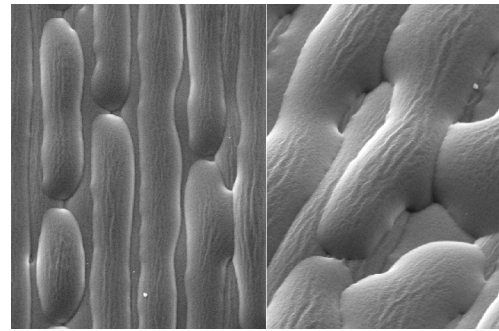


Figure 10: Solidified pixels on the transfer drum prior to transfixing.

Note the lack of coalescence of some droplets, partial coalescence of others, and full coalescence of others. Clearly, the degree of coalescence depends on the thermal conditions of the system, the time delay between deposition of adjacent droplets, and the size of the droplets. If adjacent droplets do not land on the receiver in the expected location either by printhead jetting error or motion control error, droplet coalescence is affected. Similarly, if the drop deposition algorithm (halftoning) changes, coalescence may be affected. Note the directional dependence of the coalescence in Figure 10 due to the pixel placement jet-to-jet time scale relative to the pixel placement line-to-line time scale.

In addition to these factors, it must be noted that surface features of the media play a key role in successful transfix and ultimate image quality and durability of the final image. To give the reader a feel for this dependence on the media surface, Figure 11 presents SEM images of transfixed single ink droplets on Hammermill Laser Print paper.

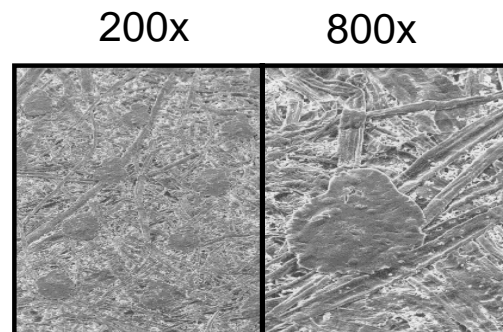


Figure 11: Transfixed single ink droplets on Hammermill Laser Print paper.

In conclusion, the solid-ink offset printing process is relatively young in its development as compared to many other competitive technologies; however, it possesses many inherent and overwhelming advantages over its competitors. Proof of these advantages is the success of the Tektronix Phaser® 350 printer, which currently sells at the top of the networked office color printing class. Also, a medical diagnostic printer is currently under development jointly by

Tektronix Inc. and Sterling Diagnostic Imaging. Field evaluations at several hospitals and clinics confirm full diagnostic image quality and equivalence to conventional wet-processed silver halide laser recording systems (Apple et al., 1997). Other applications are possible in the graphic arts, wide format, and short run markets.

Acknowledgements

Special thanks to all the people at Tektronix who spent personal time to help make this paper possible, especially the printhead component development group. Also, credit must be given to Clark Crawford and Mark Fondrk for the development of the mechanical nip model.

References

1. L.V. Bui, D.R. Titterington, J.D. Rise, C.W. Jeager, J.C. Mutton, H.P. Lee, Imaging Process, U.S. Patent 5389958.
2. D.R. Titterington, L.V. Bui, L.M. Hirschy, H.R. Frame, Indirect printing process for applying selective phase change ink compositions to substrates, U.S. Patent 5372852.
3. C.W. Spehrley, Jr., Spectra Inc., SPIE Vol. 2171, 1992.
4. B.A. Apple, M.H. Tennant, J.T. Thomas, Jr., "Novel hard copy system for digital medical imaging," Proc SPIE 3018, 1997.